Generation of acoustic vortices in crystals by conical electric field: a collinear acousto-optic diffraction

Mys O., Vasylkiv Yu., Adamenko D., Kostyrko M., Skab I. and Vlokh R.

O. G. Vlokh Institute of Physical Optics, 23 Dragomanov Street, 79005 Lviv, Ukraine; vlokh@ifo.lviv.ua

Received: 20.09.2022

Abstract. We consider topological defects of orientation of the eigenvectors of Christoffel tensor, which appear in the external conically shaped electric field. It is shown that the conical electric field applied along the principal Z axis in $LiNbO_3$ crystals produces a conical distribution of the phase difference of acoustic waves (AWs), with a zero phase difference occurring in the centre of the acoustic beam, and gives rise to a topological defect of orientation of the eigenvectors of the Christoffel tensor, with the defect strength equal to –½. We also consider a backward collinear acousto-optic diffraction under the conditions when either circularly or linearly polarized incident optical waves interact with a circularly polarized excited AW. In the first case, the diffracted optical wave bears a doubly charged optical vortex, with summing up of the charges of the AW and the optical vortex wave. When the signs of the charges of the vortices carried by interacting AW and optical wave are opposite, the diffracted wave is vortex-free, since the charges of the vortices of the incident optical wave and the AW are cancelled. In the second case of the linearly polarized incident optical wave, a vector beam with the unit polarization order is generated in the crystals. The acousto-optic interaction of this vector beam with the acoustic beam bearing a singly charged vortex results in a vortex-bearing diffracted optical wave. The strength of the embedded topological defect of the phase front for this wave represents a sum of the strengths of the topological defects referred to the incident optical wave and the AW. The diffracted optical beam represents a beam with isotropic vortex with the orbital angular momentum equal to $-2\hbar$.

Keywords: acoustic vortex, optical vortex, conical electric field, collinear acousto-optic diffraction

UDC: 535.012+534.2

1. Introduction

It is known that the velocities v_{qp} of acoustic waves (AWs) can be calculated using the Christoffel equation and the elastic-stiffness coefficients C_{ijkl}:

$$C_{ijkl} m_j m_k p_l = \rho v_{qp}^2 p_i . \quad (1)$$

Here the indices q and p correspond respectively to the propagation and polarization directions of the AW, m_j and m_k are the wavevector components of this wave, while p_l and p_i imply the components of its polarization (see, e.g., Ref. [1]). The product $C_{ijkl} m_j m_k = M_{il}$ in Eq. (1) defines the second-rank Christoffel tensor M_{il}.

In piezoelectric materials, the AW velocities can be changed due to the effect of electric polarization induced by the mechanical strains which are caused by the AW. In this case, Eq. (1) can be rewritten as

$$\left(M_{il} + \frac{4\pi}{K} g_i g_l \right) p_l = \rho v_{qp}^2 p_i , \tag{2}$$

where $g_i = e_{jik} m_j m_k$ and $g_l = e_{jlk} m_j m_k$ are the vectors that form a dyadic product in Eq. (2), e_{jik} and e_{jlk} mean the piezoelectric tensors, $K = \varepsilon_{jk} m_j m_k$ represents a scalar, and ε_{jk} denotes the dielectric permittivity. As a result, the AW velocities can be determined by a general relation

$$v \approx v_0 \left(1 + \frac{1}{2} \frac{4\pi e_{jik} e_{jlk}}{\varepsilon_{jk} C_{ijkl}} \right), \tag{3}$$

where v_0 is the AW velocity with no account for the piezoelectric contribution.

Hence, the electric polarization induced by the AW leads to a change in the velocity of this wave. As a consequence, the effect of change in the AW velocity caused by a bias electric field should also exist. In fact, this effect (referred to as an electro-acoustic effect) has been revealed by K. Hruska [2–5] in 1961 as a change in the resonant frequencies of quartz resonators occurring under a bias electric field. With a standard matrix notation used for the elastic stiffnesses or compliances (e.g., $C_{ijkl} = C_{mn}$), this effect has been described phenomenologically as changes in the compliance ($\Delta S_{rs} = S_{rs}^0 \big|_{E_t=0} - S_{rs} \big|_{E_t \neq 0}$) or stiffness ($\Delta C_{rs} = C_{mn}^0 \big|_{E_t=0} - C_{mn} \big|_{E_t \neq 0}$) coefficients occurring under the electric field:

$$\Delta S_{rs} = \psi_{rst} E_t , \; \Delta C_{mn} = \vartheta_{mnt} E_t , \tag{4}$$

with ψ_{rsl} and ϑ_{mnl} being polar fifth-rank tensors with the internal symmetry [[V^2]^2]V and E_t denoting the electric-field components. The tensor components ψ_{rsl} have been determined experimentally for the α-quartz crystals. It is known that they have the order of magnitude 10^{-23}–10^{-22} N^{-1}V^{-1}m^3 [4]. Therefore the tensor ϑ_{mnt}, which can be calculated as $\vartheta_{mnt} = C_{mn}^0 C_{rs}^0 \psi_{rst}$, has the order of the magnitude 10^0–10^3 Nm^{-1}V^{-1}. {We remind also that the electro-acoustic effect can be large enough in ferroelectric relaxors [6].}

Let us notice that the electro-acoustic effect is analogical to a well-known electro-optic Pockels effect in crystal optics. The latter effect implies that a bias electric field can change the speed of light in crystalline materials or, what is the same, the refractive indices of these materials. Due to evident symmetry limitations, both effects can exist only in non-centrosymmetric material media. It is worthwhile that the electric field as a polar-vector action lowers the symmetry of crystals. Then the acoustic axes can become split in the external electric field [7]. This phenomenon is analogical to splitting of an optical axis in crystal optics in the external electric field, which occurs due to reduced symmetry corresponding to a transition from optically uniaxial state to optically biaxial one.

The electro-acoustic effect has been experimentally studied for a number of crystals [8]. It can have applications in such fields as, e.g., acoustic-delay lines, electrostatic voltage measurements [7] and micro-electro-mechanical systems [9]. In the present work, we are interested in the electro-acoustic effect from the viewpoint of possible generation of topological defects of the eigenvectors of the Christoffel tensor by the electric field. This could result in acoustic vortices produced by the external electric fields in crystals.

It has been shown in our recent studies [10, 11] that the electric field conically distributed in space can induce a topological defect of optical-indicatrix orientation due to electro-optic Pockels and Kerr effects. This produces singly or doubly charged optical vortices. In the present work we

analyze a possible generation of acoustic vortices in the crystals subjected to a conically distributed electric field via the electro-acoustic effect. We will also analyze a collinear acousto-optic (AO) interaction between the acoustic and optical vector-vortex beams generated by the conically distributed electric field.

2. Methods of analysis

Fundamentals of the method used for the analysis of optical-vortex generation via application of conical electric fields to crystals has been described in our recent work [10]. For convenience, in the present study we will use the same parameters as those reported in Ref. [10]. The analysis will be carried out on the example of $LiNbO_3$ crystals belonging to the point symmetry group 3*m* (with the symmetry plane *m* being perpendicular to the crystallographic axis *X*, i.e. $m \perp X$). The acoustic axes of lithium niobate are parallel to the three-fold symmetry axis (i.e., to the principal axis *Z*). The quasi-transverse AWs QT_1 and QT_2 with the orthogonal polarizations propagate along this axis with the same velocities (3574 m/s [12]). The other basic parameters needed for our calculations have earlier been reported in Ref. [12]. In particular, the elastic-stiffness coefficients of lithium niobate written in the matrix notation under the conditions of constant electric field are as follows: $C_{11} = 203.0$, $C_{12} = 57.3$, $C_{13} = 75.2$, $C_{33} = 242.4$, $C_{14} = 8.5$, $C_{44} = 59.5$ and $C_{66} = 72.8$ GPa. The crystal density is equal to $\rho = 4640\ \mathrm{kg/m^3}$, whereas the ordinary and extraordinary refractive indices are equal respectively to $n_o = 2.286$ and $n_e = 2.203$ (at the light wavelength $\lambda = 632.8$ nm).

A crystal sample with electrical contacts of different diameters is sketched in Fig. 1. The radius of a smaller contact is taken to be equal to 0.1 mm, the radius of the larger one is $R = 10$ mm, and the sample thickness is equal to $d = 5$ mm. A transverse AW in the GHz frequency range can probably be excited using a thin-film piezoelectric transducer (see, e.g., Ref. [13]), while a linearly polarized AW can be transformed into a circularly polarized one with the aid of an acoustic quarter-wave plate [14]. Here we assume that the frequency of the excited AW is equal to $f_{ac} = 5$ GHz and the voltage applied to the crystal amounts to $U = 5000$ V.

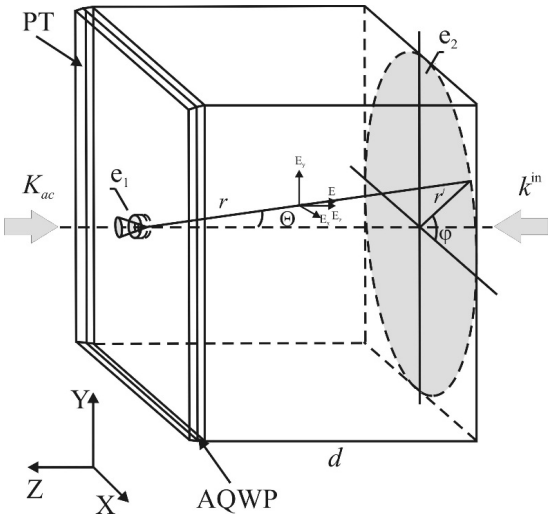

Fig. 1. Scheme of a crystalline plate with circular electrodes e_1 and e_2 producing a conical spatial distribution of the electric field. The coordinate axes *X*, *Y* and *Z* are parallel to the eigenvectors of Fresnel ellipsoid, PT is a piezoelectric transducer, AQWP an acoustic quarter-wave plate with the holes for applying electric fields, and *d* implies the sample thickness.

When the contacts differ essentially by their radiuses (e.g., the radius of one of them tends to zero), the two projections $E_1 = E_x$ and $E_2 = E_y$ of the electric field would appear. Then the electric-field components are given by the relations

$$E_1 = kX\ ,\ E_2 = kY\ ,\ E_3 = kZ\ , \tag{5}$$

where

$$k = \frac{U}{d}\frac{Z}{X^2 + Y^2 + Z^2}\ . \tag{6}$$

In the spherical coordinate system defined by the relations $X = r\sin\Theta\cos\varphi$, $Y = r\sin\Theta\sin\varphi$ and $Z = r\cos\Theta$, we obtain

$$E_1 = \frac{U}{d}\frac{\tan\Theta}{1+\tan^2\Theta}\cos\varphi\ , \tag{7}$$

$$E_2 = \frac{U}{d}\frac{\tan\Theta}{1+\tan^2\Theta}\sin\varphi\ , \tag{8}$$

$$E_3 = \frac{U}{d(1+\tan^2\Theta)}\ , \tag{9}$$

with $E_0 = U/d$. One can see that the E_1 and E_2 components are equal to zero when $\Theta = 0$ (the case of a homogeneous field with the field lines being parallel to the *Z* axis). These components increase with increasing Θ and decreasing *d*. Notice also that we neglect the electric field appearing behind the cone, which is limited by the filed lines.

According to Ref. [15], the fifth-rank tensor with the internal symmetry $[[\mathrm{V}^2]^2]\mathrm{V}$ contains 13 independent components for the point symmetry 3*m*: ϑ_{151}, ϑ_{161}, ϑ_{251}, ϑ_{261}, ϑ_{351}, ϑ_{361}, ϑ_{451}, ϑ_{113}, ϑ_{123}, ϑ_{133}, ϑ_{143}, ϑ_{333} and ϑ_{443}. The other coefficients can be expressed as $\vartheta_{461} = (\vartheta_{151} + \vartheta_{251})/2$, $\vartheta_{112} = (\vartheta_{161} + 3\vartheta_{261})/2$, $\vartheta_{122} = (\vartheta_{161} - \vartheta_{261})/2$, $\vartheta_{132} = \vartheta_{361}$, $\vartheta_{142} = \vartheta_{251}$, $\vartheta_{222} = -(3\vartheta_{161} + \vartheta_{261})/2$, $\vartheta_{232} = -\vartheta_{361}$, $\vartheta_{242} = \vartheta_{151}$, $\vartheta_{342} = \vartheta_{351}$, $\vartheta_{442} = -\vartheta_{451}$, $\vartheta_{552} = \vartheta_{451}$, $\vartheta_{562} = (\vartheta_{151} - \vartheta_{251})/2$, $\vartheta_{662} = (\vartheta_{161} - \vartheta_{261})/2$, $\vartheta_{223} = \vartheta_{113}$, $\vartheta_{233} = \vartheta_{133}$, $\vartheta_{243} = -\vartheta_{341}$, $\vartheta_{563} = -\vartheta_{143}$, $\vartheta_{663} = (\vartheta_{113} - \vartheta_{123})/2$ and $\vartheta_{553} = \vartheta_{451}$. On the other hand, we have the equality $C_{44} = C_{55}$ for the elastic-stiffness coefficients, which is valid for the crystals of the point group 3*m*. Moreover, the crystal symmetry remains the same under the electric field applied along the *Z* axis. These conditions lead to the additional relations $\vartheta_{553} = \vartheta_{443} = \vartheta_{451}$. Then the components of the Christoffel tensor under the conical electric field can be written as $M_{11} = C_{44} + \vartheta_{451}(E_2 + E_3)$, $M_{22} = C_{44} - \vartheta_{451}(E_2 - E_3)$, $M_{33} = C_{33} + \vartheta_{333}E_3$, $M_{23} = \vartheta_{351}E_2$, $M_{31} = \vartheta_{351}E_1$ and $M_{12} = \vartheta_{451}E_1$.

The electro-acoustic coefficient needed by us has been determined in Ref. [16]: $\vartheta_{451} = 20.3\ \mathrm{Nm^{-1}V^{-1}}$. According to Refs. [15, 17], the coefficient ϑ_{443} is either $-10.2\ \mathrm{Nm^{-1}V^{-1}}$ or $-3\ \mathrm{Nm^{-1}V^{-1}}$. Since the corresponding errors are very high, we will use only the electro-acoustic coefficient $\vartheta_{451} = 20.3\ \mathrm{Nm^{-1}V^{-1}}$ in our further calculations. The angle of rotation of the eigenvectors of the Christoffel tensor around the *Z* axis is given by

$$\tan 2(\zeta_Z)_{ac} = \frac{2M_{12}}{M_{11} - M_{22}} = \frac{E_1}{E_2} = \frac{\cos\varphi}{\sin\varphi} = \cot\varphi\ , \tag{10}$$

i.e. we have

$$(\zeta_Z)_{ac} = \frac{1}{2}\arctan(\cot\varphi) = \pi/4 - \varphi/2\ . \tag{11}$$

Following from Eq. (11), one can state that the topological defect of eigenvectors of the Christoffel tensor has the strength equal to $q_{ac} = -½$, while the acoustic vortex generated by this topological defect is isotropic and singly charged. Under the voltage equal to 5×10^3 V, the angles of rotation of the eigenvectors of the Christoffel tensor around the *X* and *Y* axes (i.e., the angles of acoustic non-orthogonality) are quite small ($\sim 3\times10^{-3}$ deg), so that one can neglect these angles. Using the components of the Christoffel tensor, one can obtain the following velocities of the transverse AWs propagating along the *Z* axis:

$$v_{31} = \sqrt{\frac{2C_{44} + 2\vartheta_{451}E_3 + 2\vartheta_{451}\sqrt{{E_2}^2 + E_1^2}}{2\rho}}\ ,\ v_{32} = \sqrt{\frac{2C_{44} + 2\vartheta_{451}E_3 - 2\vartheta_{451}\sqrt{{E_2}^2 + E_1^2}}{2\rho}}\ . \quad (12)$$

Then the AW velocity difference is given by

$$\Delta v = v_{31} - v_{32} = \frac{\vartheta_{451}}{\sqrt{\rho}}\sqrt{\frac{{E_2}^2 + E_1^2}{C_{44} + \vartheta_{451}E_3}}\ . \quad (13)$$

For a homogeneous crystal sample with the thickness d_h, the phase difference between these transverse AWs reads as

$$\Delta\Gamma_{ac} = 2\pi f_{ac} d_h \left(\frac{1}{v_{31}} - \frac{1}{v_{32}}\right). \quad (14)$$

Assuming a spatially inhomogeneous character of a crystal subjected to an inhomogeneous electric field, one can divide this crystal into a (relatively large) number of homogeneous elementary cells. The acoustic phase difference between the AWs in each elementary cell can be written as

$$(\Delta\Gamma_{ij}^n)_{ac} = 2\pi d_{ij}^n f_A \frac{4\sqrt{\rho}\vartheta_{451}\sqrt{\left({E_2}^2 + E_1^2\right)\left(\mathrm{C}_{44} + \vartheta_{451}E_3\right)}}{4(\mathrm{C}_{44} + \vartheta_{451}E_3)^2 - \vartheta_{451}^2({E_2}^2 + E_1^2)}, \quad (15)$$

where the index *n* corresponds to the homogeneous layer perpendicular to the *Z* axis. Each layer is divided into $i\times j$ elementary cells and d_{ij}^n denotes the thickness of the elementary cell along the *Z* direction. In our simulations, we put $n_{\max} = 1 \div 100$, $i = 200$ and $j = 200$.

Supposing that the AWs are purely transverse, one can apply the Jones matrix approach when calculating the integrated phase difference and the orientations of the eigenvectors of the Christoffel tensor. The resulting Jones matrix for each elementary acoustic beam can be presented as

$$J_{ij} = \prod_{n=1}^{n_{\max}} J_{ij}^n = \prod_{n=1}^{N_{\max}} \begin{vmatrix} \left(e^{\frac{i\left(\Delta\Gamma_{ij}^n\right)_{ac}}{2}}\cos^2\left(\zeta_{ij}^n\right)_{ac} + e^{-i\Delta\Gamma_{ij}^n/2}\sin^2\left(\zeta_{ij}^n\right)_{ac}\right) & i\sin\left(\frac{(\Delta\Gamma_{ij}^n)_{ac}}{2}\right)\sin 2\left(\zeta_{ij}^n\right)_{ac} \\ i\sin\left(\frac{\left(\Delta\Gamma_{ij}^n\right)_{ac}}{2}\right)\sin 2\left(\zeta_{ij}^n\right)_{ac} & \left(e^{\frac{i\left(\Delta\Gamma_{ij}^n\right)_{ac}}{2}}\sin^2\left(\zeta_{ij}^n\right)_{ac} + e^{-i(\Delta\Gamma_{ij}^n)_{ac}/2}\cos^2\left(\zeta_{ij}^n\right)_{ac}\right) \end{vmatrix}, \quad 6)$$

where $(\zeta_{ij}^n)_{ac} = \frac{1}{2}\arctan\frac{X}{Y}$ is the rotation angle of the eigenvectors of the Christoffel tensor within the elementary cell. As a result, the integrated phase difference for each elementary acoustic beam reads as

$$(\Delta\Gamma_{ij})_{ac} = 2\ \arccos(\mathrm{Re}[J_{ij}]_{(d)})\ . \quad (17)$$

Then the integrated orientation angles of the eigenvectors of the Christoffel tensor are given by

$$(\zeta_{ij})_{ac} = \frac{1}{2}\arcsin\left(\frac{\mathrm{Im}(J_{ij})_{(nd)}}{\sin\left(\frac{\Delta\Gamma_{ij}^{n}}{2}\right)}\right), \tag{18}$$

where the indices (*d*) and (*nd*) indicate the diagonal and non-diagonal components of the Jones matrix, respectively.

3. Results and discussion

The results concerned with the topological defects of optical-indicatrix orientation and the generation of optical vortices due to the Pockels effect have been described in detail in our work [10]. The experimental conditions taken in Ref. [10] have been the same as those described above for acoustics. As a consequence, we will omit the procedures that ensure derivation of the results in this work. We remind only that the strength of the topological defect of the optical-indicatrix orientation produced by the conically shaped electric field due to the Pockels effect is equal to $q_{op} = -½$, while the corresponding optical vortex has a unit charge.

The spatial distributions of the phase difference for the AWs and the orientations of the eigenvectors of the Christoffel tensor calculated for the $LiNbO_3$ crystals are presented in Fig. 2. In the region close to the beam centre, the distribution of the phase difference is conical, with a zero value occurring in the centre (see Fig. 2a). The eigenvectors of the Christoffel tensor rotate in the opposite directions with respect to the change in the azimuthal angle φ (see Fig. 2b). Thus, the strength of the topological defect associated with the orientation of eigenvectors of the Christoffel tensor is equal to $q_{ac} = -½$.

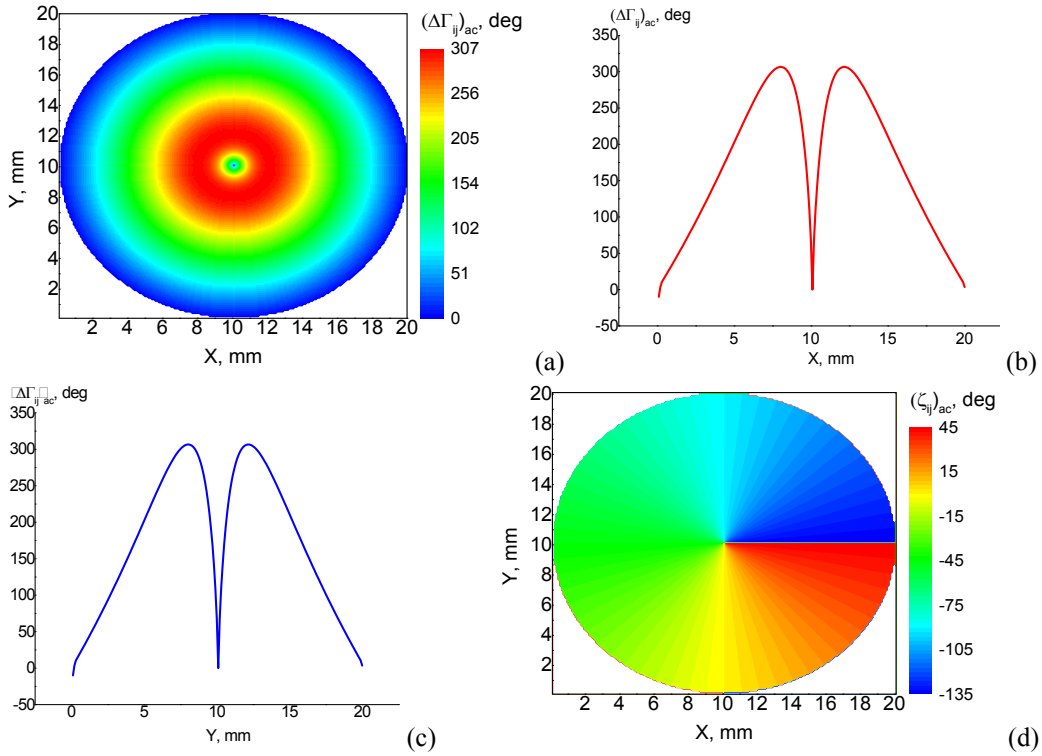

Fig. 2. *XY*-distribution of the AW phase difference (panel a) and its central profiles (panels b and c), and *XY*-distribution of orientation of the eigenvectors of the Christoffel tensor (panel d), as calculated for lithium niobate at f_{ac} = 5 GHz and the electrical voltage U = 5000 V.

Upon emerging from the $LiNbO_3$ crystals, a right-handed (RH) circularly polarized AW, for which a spin angular momentum is equal to $\hbar$, would propagate along the Z axis. Inside the crystalline sample, two AWs propagate. The first one is a vortex-free AW with the same sign of its circular polarization as the incident one. The second AW bears a singly charged acoustic vortex (with the orbital angular momentum being equal to $l = 2q_{ac} = -1$) and has the opposite sign of the circular polarization (and the spin angular momentum equal to $-\hbar$). The process of splitting of the circularly polarized AW into the two modes is the same as in optics (see, e.g., Ref. [18]). Therefore, the appropriate analysis applied to the case of the incident circularly polarized optical wave should also be valid in our case. As a result, we state that the incident circular (RH) Gaussian acoustic beam with a small divergence can be described by the displacement vector

$$u^{RH} = u_0 \begin{bmatrix} 1 \\ i \end{bmatrix} e^{i(\Omega t - K_{ac} Z)}, \tag{19}$$

where Ω is the frequency of the AW, K_{ac} its wavevector, and u_0 denotes the unit amplitude of the displacement vector. Note that the RH polarization is accepted for the case of clockwise rotation of the displacement vector, provided that the observation direction is opposite to K_{ac} (see Ref. [19] where a similar situation has been considered for the case of optics).

When the conical electric field is applied along the Z axis (i.e., the cone axis is parallel to the Z axis), an 'acoustic birefringence' and a topological defect of the eigenvectors of the Christoffel tensor would appear. Now let us consider a particular case of a backward collinear AO diffraction (see Fig. 3). Here a linearly polarized incident optical wave with the polarization parallel to the X axis diffracts by the AW bearing the acoustic vortex. [Note that the relations obtained for the optical wave with the polarization parallel to the Y axis are similar to those displayed below.] The displacement vector of the AW bearing the vortex can be described as follows:

$$u^{LH} = u_0 \sin \frac{(\Delta\Gamma_{ij})_{ac}(r', E)}{2} \begin{bmatrix} 1 \\ -i \end{bmatrix} e^{i(2q_{ac}\varphi + 2(\zeta_Z^0)_{ac}) + i(\Omega t - K_{ac} Z)}, \tag{20}$$

where $(\zeta_Z^0)_{ac}$ denotes the orientation angle of the eigenvectors of the Christoffel tensor at $\varphi = 0$ (in our case $(\zeta_Z^0)_{ac} = \pi / 4$) and E implies the acting electric field. The strain-tensor components caused by this AW can be represented as

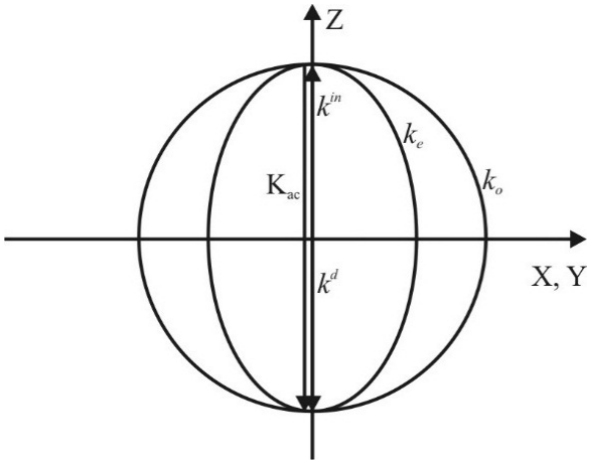

Fig. 3. A schematic view of phase-matching condition provided at a backward collinear diffraction: k^{in} and k^d are the wavevectors of the incident and diffracted optical waves, and k_o and k_e denote the wavevectors of the ordinary and extraordinary optical waves.

$$e_4 = 2e_{23} = \left(\frac{\partial u_2}{\partial Z} + \frac{\partial u_3}{\partial Y}\right) = -K_{ac} e_0 \sin\frac{(\Delta\Gamma_{ij})_{ac}(r', E)}{2} e^{2iq_{ac}\varphi + i\pi/2 + i(\Omega t - K_{ac} Z)},$$
$$e_5 = 2e_{13} = \left(\frac{\partial u_1}{\partial Z} + \frac{\partial u_3}{\partial X}\right) = -iK_{ac} e_0 \sin\frac{(\Delta\Gamma_{ij})_{ac}(r', E)}{2} e^{2iq_{ac}\varphi + i\pi/2 + i(\Omega t - K_{ac} Z)}, \quad (21)$$

with e_0 being the unit strain.

The linearly polarized incident optical waves with their polarizations parallel to the X axis can be described by the state vectors

$$D_1^{in} = D_o \begin{pmatrix} 1 \\ 0 \end{pmatrix} e^{i(\omega t + k^{in} Z)}, \quad (22)$$

where D_0 is the unit electric-induction amplitude, k^{in} the wavevector of the incident optical wave, and ω its frequency. As a result of the singularity induced by the conical electric field, the Jones matrix of the perturbed material medium acquires the following form (see Ref. [17]):

$$M(X,Y) = \cos\frac{(\Delta\Gamma_{ij})_{op}(r', E)}{2} \begin{bmatrix} 1 & 0 \\ 0 & 1 \end{bmatrix} + i \sin\frac{(\Delta\Gamma_{ij})_{op}(r', E)}{2} \begin{bmatrix} \cos 2(\zeta_Z)_{op} & \sin 2(\zeta_Z)_{op} \\ \sin 2(\zeta_Z)_{op} & -\cos 2(\zeta_Z)_{op} \end{bmatrix}, \quad (23)$$

where $(\Delta\Gamma_{ij})_{op}(r', E) = 2\pi\Delta n^{eff}(r', E) d / \lambda$ is the field-induced optical phase difference, Δn^{eff} the effective birefringence, λ the wavelength of optical radiation, and $(\zeta_Z)_{op} = -\varphi/2 = q_{op}\varphi$ the field-induced optical-indicatrix rotation angle which is counted around the Z axis [10]. Thus, we have a topological defect of the optical-indicatrix orientation with the strength equal to $q_{op} = -½$. The incident X-polarized optical wave can be decomposed inside the crystal:

$$D(X,Y) = D_0 \cos\frac{(\Delta\Gamma_{ij})_{op}(r', E)}{2} \begin{bmatrix} 1 \\ 0 \end{bmatrix} e^{i(\omega t + k^{in} Z)} + iD_0 \sin\frac{(\Delta\Gamma_{ij})_{op}(r', E)}{2} \begin{bmatrix} \cos 2(\zeta_Z)_{op} \\ \sin 2(\zeta_Z)_{op} \end{bmatrix} e^{i(\omega t + k^{in} Z)}. \quad (24)$$

The second term in the r. h. s. of Eq. (24) describes the optical vector beam with the unit polarization order.

As a result, the electric-field components of the diffracted wave can be written as

$$E^d = -ip_{14} \sin\frac{(\Delta\Gamma_{ij})_{op}(r', E)}{2} \sin\frac{(\Delta\Gamma_{ij})_{ac}(r', E)}{2} \begin{bmatrix} 1 \\ i \end{bmatrix} e^{i\left[2q_{ac}\varphi + 2q_{op}\varphi + \pi/2 + [\omega + \Omega]t + [k^{in} - K_{ac} Z]\right]}, \quad (25)$$

where p_{14} denotes the elasto-optic coefficient. Note that the parameters D_0 and e_0 and the corresponding unit parameter referred to K_{ac} are not written down in the above equations for the reasons of brevity. One can see that the diffracted optical wave represents a circularly polarized RH wave. It contains a topological defect of the phase front with the strength equal to the sum of strengths of the defects associated with the optical and acoustic waves: $q^d = (q_{ac} + q_{op})\varphi = -1$. Hence, the diffracted wave bears a doubly charged optical vortex with the orbital angular momentum equal to $-2\hbar$.

Now let us consider the backward collinear AO interaction with the incident circularly polarized optical wave having the RH polarization,

$$D^{RH} = D_0 \begin{bmatrix} 1 \\ i \end{bmatrix} e^{i(\omega t + k^{in} Z)}. \tag{26}$$

The electric induction at the output plane of the crystal can be described as a sum of two terms:

$$\begin{aligned} D(\rho, E) = D_0 \cos \frac{(\Delta\Gamma_{ij})_{op}(r', E)}{2} \begin{bmatrix} 1 \\ i \end{bmatrix} e^{i(\omega t + k^{in} Z)} \\ + iD_0 \sin \frac{(\Delta\Gamma_{ij})_{op}(r', E)}{2} \begin{bmatrix} 1 \\ -i \end{bmatrix} e^{-2iq_{op}\varphi + i(\omega t + k^{in} Z)} \end{aligned}. \tag{27}$$

The first term in the r. h. s. of Eq. (27) describes the wave that remains the same as the incident one. On the contrary, the second term represents a left-handed circular wave bearing a singly charged vortex.

The electric field of the diffracted wave also involves two components:

$$\begin{aligned} E_1^d = \Delta B_{11} D_1^{in} + \Delta B_{12} D_2^{in} = -i2 p_{14} K_{ac} \sin \frac{(\Delta\Gamma_{ij})_{ac}(r', E)}{2} \\ \times \sin \frac{(\Delta\Gamma_{ij})_{op}(r', E)}{2} e^{-i4q\varphi + i\pi/2 + i(\omega + \Omega)t + i(k^{in} - K_{ac})Z} \end{aligned}, \tag{28}$$

$$\begin{aligned} E_2^d = \Delta B_{22} D_2^{in} + \Delta B_{21} D_1^{in} = 2 p_{14} K_{ac} \sin \frac{(\Delta\Gamma_{ij})_{ac}(r', E)}{2} \\ \times \sin \frac{(\Delta\Gamma_{ij})_{op}(r', E)}{2} e^{-i4q\varphi + i\pi/2 + i(\Omega + \omega)t + i(k^{in} - K_{ac})Z} \end{aligned}, \tag{29}$$

where $q = q_{op} = q_{ac}$. Then the resulting electric-field strength of the diffracted wave is given by

$$\begin{aligned} E^d = \sqrt{(E_1^d)^2 + (E_2^d)^2} = 2 p_{14} K_{ac} \sin \frac{(\Delta\Gamma_{ij})_{ac}(r', E)}{2} \\ \times \sin \frac{(\Delta\Gamma_{ij})_{op}(r', E)}{2} e^{-i4q\varphi + i\pi/2 + i(\Omega + \omega)t + i(k^{in} - K_{ac})Z} \end{aligned}. \tag{30}$$

As seen from Eq. (30), the diffracted wave bears a doubly charged optical vortex. In other words, the charges of the vortices referred to the acoustic and optical waves are summed up. It is also obvious that the signs of charges of the vortices carried by the interacting acoustic and optical waves are different whenever these waves have the opposite chiralities. Then the diffracted wave is vortex-free since the charges of the vortices of the incident optical and acoustic waves are cancelled out. Note also that the scenario described above is the same as that observed earlier for the case of crystals subjected to torsion [20].

Finally, let us notice that the effects analyzed in this work can exist in any crystals that belong to the symmetry groups 3*m*, 32, 3, 23 and $\bar{4}$3m , provided that the conically shaped electric field is applied along the three-fold symmetry axis.

4. Conclusions

In the present work, we have considered the topological defect of orientation of the eigenvectors of the Christoffel tensor, which arises in the conically shaped external electric field. The corresponding mechanism is the changes occurring in the velocities of transverse AWs, which are induced by the electro-acoustic effect. It has been shown that the conical electric field applied along the principal *Z* axis of lithium niobate produces a conical spatial distribution of the AW phase difference, with a zero phase difference in the acoustic-beam centre. At the same time, the eigenvectors of the Christoffel tensor are rotated around the beam centre by the angle equal to $-\pi$

whenever the azimuthal angle is changed by 2π. This corresponds to the topological defect of orientation of the eigenvectors of the Christoffel tensor with the strength equal to –½ and the singular value of the AW phase difference.

The backward collinear AO diffraction has been considered under the conditions when the circularly and linearly polarized incident optical waves interact with the circularly polarized AW. In the first case we deal with the AO interaction of the acoustic vortex beam with the optical vortex beam generated by the conical electric field. It has been shown that the diffracted wave in this case bears the doubly charged optical vortex. In other words, the charges of the vortices referred to the acoustic and optical waves are summed up. When the signs of charges of the vortices carried by the interacting acoustic and optical waves are different, then the diffracted wave is vortex-free, since the charges of the vortices of the incident optical wave and the AW are compensated.

We have also shown that, in the case of incident linearly polarized optical wave, a vector beam with the unit polarization order is generated in the crystals. The AO interaction of this vector beam with the acoustic beam bearing a singly charged vortex results in a vortex-bearing diffracted optical wave. The strength of the embedded topological defect of the phase front for this wave is a sum of the strengths of the topological defects referred to the incident optical wave and the AW. The diffracted optical beam represents an isotropic vortex beam with the orbital angular momentum equal to $-2\hbar$.

Acknowledgement. The authors acknowledge the Ministry of Education and Science of Ukraine for financial support of the present study (the Project #0120U102031).3

References

1. Sirotin Y I and Shaskolskaya M P. Fundamentals of crystal physics. Moscow: Nauka, 1975.
2. Hruska K, 1961. The influence of an electric field on the frequency of the piezoelectric cuts. Czech. J. Phys. B. **11**: 150–152.
3. Hruska K, 1962. An attempt at a phenomenological interpretation of the influence of the polarizing field on the piezoelectric resonator. Czech. J. Phys. B. **12**: 338–353.
4. Hruska K, 1963. Tensor of polarizing correction terms of quartz elastic coeficients. Czech. J. Phys. B **13**: 307–308.
5. Hruska K and Janik L, 1968. Change in elastic coefficients and moduli of α-quartz in an electric field. Czech. J. Phys. B. **18**: 112–116.
6. Leary S P and Pilgrim SM, 1998. Measuring the electric field dependence of the elastic moduli of $Pb(Mg_{1/3}Nb_{2/3})O_3$ relaxor ferroelectitric. ISAF 98. Proceedings of the Eleventh International Symposium on Applications of Ferroelectrics. IEEE, pp. 451–454.
7. Zaitsev B D and Kuznetsova I E, 1998. Behavior of acoustic axes and internal conical refraction in $LiNbO_3$ and $SrTiO_3$ crystals placed in an external electric field. IEEE Trans. Ultrason. Ferroel. Freq. Contr. **45**: 361–366.
8. Zaitsev B D and Kuznetsova I E, 2001. In: Electric field influence on acoustic waves. Handbook of Advanced Electronic and Photonic Materials and Devices. Ferroelectrics and Dielectrics. Ed. by H. S. Nalwa. Vol. 4, pp. 139–173.
9. Kuypers J H, Schmidt M E, Tanaka S and Esashi M, 2007. Phase velocity control of surface acoustic waves based on surface shorting and electrical field application using MEMS switches. 2007 IEEE Ultrasonics Symposium, pp. 1233–1238.
10. Skab I, Vasylkiv Yu, Smaga I and Vlokh R, 2011. Spin-to-orbital momentum conversion via electro-optic Pockels effect in crystals. Phys. Rev. A. **84**: 043815.

11. VasylkivY, Skab I and Vlokh R, 2014. Generation of double-charged optical vortices on the basis of electro-optic Kerr effect. Appl. Opt. **53**: B60–B73.
12. Smith R T and Welsh F S, 1971. Temperature dependence of the elastic, piezoelectric, and dielectric constants of lithium tantalate and lithium niobate. J. Appl. Phys. **42**: 2219–2230.
13. Jakob A, Bender M, Knoll T, Lemor R, Lehnert T, Koch M, Veith M, Zhou Q, Zhu B P, Han J X and Shung K K, 2009. Comparison of different piezoelectric materials for GHz acoustic microscopy transducers. 2009 IEEE International Ultrasonics Symposium, pp. 1722–1725.
14. Auld B A, Quate C F, Shaw H J and Winslow D K, 1966. Acoustic quarterwave plates at microwave frequencies. Appl. Phys. Lett. **9**: 436–438.
15. Zhang Y, Jin J and Hu H, 2019. Third-order elastic, piezoelectric, and dielectric constants. Appl. Math. Mech. Engl. Ed. **40**: 1831–1846.
16. Cho Y and Yamanouchi K, 1987. Nonlinear, elastic, piezoelectric, electrostrictive, and dielectric constants of lithium niobate. J. Appl. Phys. **61**: 875–887.
17. Korobov A I and Lyamov V E, 1975. Nonlinear piezoelectric coefficients of the $LiNbO_3$ crystals. Fiz. Tverd. Tela. **17**: 1448–1450.
18. Marrucci L, 2008. Generation of helical modes of light by spin-to-orbital angular momentum conversion in inhomogeneous liquid crystals. Mol. Cryst. Liq. Cryst. **488**: 148–162.
19. Azzam R M A and Bashara N M. Ellipsometry and polarized light. Amsterdam, New York: North-Holland, 1977.
20. Mys O, Kostyrko M, Adamenko D, Skab I and Vlokh R, 2022. Acoustic polarization singularities arising under torsion and orbital angular momentum exchange at the backward collinear acousto-optic diffraction: a case of crystals with point symmetry 3m. Ukr. J. Phys. Opt. **23**: 107–115.

Mys O., Vasylkiv Yu., Adamenko D., Kostyrko M., Skab I. and Vlokh R. 2022. Generation of acoustic vortices in crystals by conical electric field: a collinear acousto-optic diffraction. Ukr.J.Phys.Opt. **23**: 256 – 266. doi: 10.3116/16091833/23/4/256/2022

Анотація. *Розглянуто топологічні дефекти орієнтації власних векторів тензора Крістоффеля, які виникають у зовнішньому електричному полі конічної форми. Показано, що конічне електричне поле, прикладене вздовж головної осі Z у кристалах $LiNbO_3$, створює конічний розподіл різниці фаз акустичних хвиль (АХ), із нульовою різницею фаз у центрі акустичного пучка, і топологічний дефект орієнтації власних векторів тензора Крістоффеля із силою, що дорівнює –½. Ми також розглянули зворотну колінеарну акустооптичну дифракцію за умов, коли циркулярно або лінійно поляризовані падаючі оптичні хвилі взаємодіють із циркулярно поляризованою збудженою АХ. У першому випадку дифрагована оптична хвиля несе двозарядний оптичний вихор, а заряди АХ і оптичної вихрової хвилі сумуються. Коли знаки зарядів вихорів, що переносяться взаємодіючими АХ і оптичною хвилею, є протилежними, дифрагована хвиля безвихрова, оскільки заряди вихорів падаючої оптичної хвилі і АХ компенсуються. У разі лінійно поляризованої падаючої оптичної хвилі в кристалах генерується векторний пучок із одиничним порядком поляризації. Акустооптична взаємодія цього векторного пучка з акустичним пучком, що несе однозарядний вихор, породжує дифраговану оптичну хвилю, який переносить вихор. Сила вбудованого топологічного дефекту фазового фронту цієї хвилі представляє собою суму сил топологічних дефектів падаючої оптичної хвилі та АХ. Дифрагований оптичний пучок є пучком з ізотропним вихором, із орбітальним моментом імпульсу –2ħ.*

Ключові слова: *акустичний вихор, оптичний вихор, конічне електричне поле, колінеарна акустооптична дифракція*